LAWRENCE
LIVERMORE
NATIONAL
LABORATORY

LLNL-JRNL-652974

Lattice Anharmonicity and Thermal Conductivity from Compressive Sensing of First-Principles Calculations

F. Zhou, W. Nielson, Y. Xia, V. Ozolins

April 10, 2014

Physical Review Letters

Disclaimer

A compressive sensing approach to anharmonicity and lattice thermal conductivity

Fei Zhou(周非)
Condensed Matter and Materials Division, Lawrence Livermore National Laboratory, Livermore, California 94550, USA

Weston Nielson, Yi Xia, and Vidvuds Ozoliņš
Department of Materials Science and Engineering, University of California, Los Angeles, California 90095-1595, USA

(Dated: March 31, 2014)

A systematic information theory based approach to deriving *ab initio* Hamiltonians for lattice dynamics of crystalline materials is proposed. Compressive sensing lattice dynamics (CSLD) allows to include all anharmonic terms up to a certain order and within a certain maximum distance. The relevant terms that are necessary to reproduce the interatomic forces calculated from the density-functional theory are selected by minimizing the ℓ_1 norm of the scaled force constants. The accuracy and efficiency of the method are demonstrated for rocksalt NaCl and $Cu_{12}Sb_4S_{13}$, a recently proposed earth-abundant thermoelectric based on the natural mineral tetrahedrite.

PACS numbers: 63.20.Ry, 63.20.dk, 66.70.-f

To a large extent, thermal properties of crystalline solids are determined by the vibrations of their constituent atoms. Hence, accurate models of lattice dynamics are essential for fundamental understanding of the structure, thermodynamics, phase stability and thermal transport properties of solids. The seminal work of Born and Huang [1] forms the theoretical basis of our understanding of harmonic vibrations and their relation to elastic properties. With the advent of efficient density-functional theory (DFT) based methods for solving the Schrödinger's equation, several *ab initio* methods for studying harmonic phonon properties of solids have been proposed, such as the frozen phonon approach [2, 3], direct/small displacement method [4, 5] and the density-functional perturbation theory (DFPT) [6]. Due to these developments, DFT calculations of the harmonic phonon dispersion curves and phonon mode Grüneisen parameters have become routine.

A systematic approach to anharmonicity has been more difficult to develop. Anharmonic effects are key to explaining phenomena where finite phonon lifetimes and phonon frequency shifts? due to phonon-phonon interactions become important, such as in the study of lattice thermal conductivity κ_L and structural phase transitions. Two main theories developed to deal with such effects are the perturbation theory (PT) [7] and the self-consistent phonon (SCP) approximation [8]. For weakly anharmonic systems, phonon-phonon interactions and their effects on phonon frequencies and lifetimes can be evaluated using first-order PT [9] and lattice thermal conductivity κ_L can then be obtained by solving the Boltzmann transport equation [10]. The computational feasibility and physical accuracy of these methods are well established [11–14]. Unfortunately, PT tends to be computationally expensive for solids with large, complex unit cells, and its ability to handle strong anharmonicity is limited, especially in the cases when the harmonic phonon dispersion is already unstable. The first-principles SCP method deals with strong anharmonicity by constructing a thermally averaged effective harmonic Hamiltonian [15, 16]. Recently, SCP has been extended to calculate third-order anharmonicity in Si and FeSi [17].

Here, we introduce an efficient and general approach to building lattice dynamical models that can treat strong anharmonicity when the 3rd-order terms are insufficient (such as in the presence of harmonically unstable phonon modes) and handle compounds with large, complex unit cells. Currently, there is a dearth of methods that can be used for this purpose. The "$2n+1$" theorem of DFPT [18] gives the higher-order anharmonicity, but the required calculations are cumbersome and, to the best of our knowledge, have not been implemented for the second derivatives of wave functions, which are necessary to obtain the 4th-order anharmonic terms. The method proposed here can be implemented with any standard DFT total energy method and is expected to find applications in the study of ferroelectrics, thermoelectrics, and temperature induced structural phase transformations, including martensitic transformations.

We take an approach where the true lattice Hamiltonian is determined from the calculated DFT forces using compressive sensing (CS), a technique recently developed in the field of information science [19]. The starting point of the proposed method, compressive sensing lattice dynamics (CSLD), is a Taylor expansion of the total energy in terms of the atomic displacements,

$$V = V_0 + \Phi_{\mathbf{a}} u_{\mathbf{a}} + \frac{1}{2}\Phi_{\mathbf{ab}} u_{\mathbf{a}} u_{\mathbf{b}} + \frac{1}{3!}\Phi_{\mathbf{abc}} u_{\mathbf{a}} u_{\mathbf{b}} u_{\mathbf{c}} + \cdots \quad (1)$$

where $u_{\mathbf{a}} \equiv u_{a,i}$ is the displacement of atom a at a lattice site $\mathbf{R}_a$ in the Cartesian direction i, the 2nd-order expansion coefficients $\Phi_{\mathbf{ab}} \equiv \Phi_{ij}(ab) = \partial^2 V/\partial u_{\mathbf{a}} \partial u_{\mathbf{b}}$ determine the phonon dispersion in the harmonic approximation, and $\Phi_{\mathbf{abc}} \equiv \Phi_{ijk}(abc) = \partial^3 V/\partial u_{\mathbf{a}} \partial u_{\mathbf{b}} \partial u_{\mathbf{c}}$, etc., are third- and higher-order anharmonic force constant

tensors (FCTs). The linear term with $\Phi_{\mathbf{a}}$ is absent if the ideal lattice sites represent mechanical equilibrium. The Einstein summation convention over repeated indices is used throughout the paper. Systematic calculation (or fitting) of all the higher-order anharmonic terms is challenging not only due to combinatorial explosion in the number of tensors $\Phi(a_1 \cdots a_n)$ with increasing order n and maximum distance between the sites $\{a_1, \ldots, a_n\}$, but also due to stringent requirements on the numerical stability of the fitting procedure. Currently, fitting of higher-order anharmonic terms has been done only for relatively simple crystals and weak anharmonicity [14, 17, 20].

Direct calculations of all possible terms in Eq. (1) is not only impractical, but also unnecessary. Physical intuition suggests that the largest anharmonic terms correspond to neighboring atoms with direct chemical bonds and hence are short-ranged, while long range interactions vary slowly and can be accurately described using *harmonic* FCTs. Once the harmonic Coulomb force constants have been subtracted, the remaining interactions are expected to be short-ranged, i.e., decay faster than the 3$^{\text{rd}}$ power of the interatomic distance. Unfortunately, it is not generally obvious where to truncate the expansion (1), both with respect to distance and order. The latter requires physical intuition, which can only be gained on a case-by-case basis through time-consuming cycles of model construction and cross-validation.

We have recently shown that a similar problem in alloy theory, the cluster expansion (CE) method for configurational energetics [22, 23], can be solved efficiently and accurately using compressive sensing [24, 25]. CS has revolutionized information science by providing a mathematically rigorous recipe for reconstructing S-sparse models (i.e., models with S nonzero coefficients out of a large pool of possibles, N, when $S \ll N$) from only $O(S)$ number of data points [26–28]. Given training data, CS automatically picks out the relevant coefficients and determines their values *in one shot*. To see how this applies to lattice dynamics, we write down the force-displacement relationship for Eq. (1):

$$F_{\mathbf{a}} = -\frac{\partial V}{\partial u_{\mathbf{a}}} = -\Phi_{\mathbf{a}} - \Phi_{\mathbf{ab}} u_{\mathbf{b}} - \frac{1}{2}\Phi_{\mathbf{abc}} u_{\mathbf{b}} u_{\mathbf{c}} - \ldots . \quad (2)$$

The forces on the left hand side can be obtained from first-principles calculations using any general-purpose DFT code for a set of atomic configurations in a supercell , similar to the direct method for harmonic force constants. This establishes a linear problem for the unknown FCTs:

$$\mathbf{F} = \mathbf{A}\mathbf{\Phi}, \quad (3)$$

where the so-called sensing matrix $\mathbf{A}$ is calculated from atomic displacements according to Eq. (2). $\mathbf{A}$ is an $M \times N$ matrix, where M is the number of calculated Cartesian force components, and N is the total number of the independent, symmetrically distinct FCT elements [29]. In practice, the latter can far exceed M, which makes the linear problem Eq. (3) underdetermined. A reasonable approach would be to choose $\mathbf{\Phi}$ so that it reproduces the training data $\mathbf{F}$ to a given accuracy with the smallest number of nonzero FCTs (often called the ℓ_0 norm of the solution). Unfortunately, this is a computationally hard problem that cannot be solved in polynomial time with respect to the problem size.

CS solves the underdetermined linear problem in Eq. (3) by minimizing the ℓ_1 norm of the coefficients, $\|\mathbf{\Phi}\|_1 \equiv \sum_I |\Phi_I|$, while requiring a certain level of accuracy for reproducing the data. ℓ_1 norm serves as a computationally feasible approximation to the ℓ_0 norm and results in a tractable convex optimization problem. Mathematically, the solution is found as

$$\mathbf{\Phi}^{\text{CS}} = \arg\min_{\mathbf{\Phi}} \|\mathbf{\Phi}\|_1 + \frac{\mu}{2}\|\mathbf{F} - \mathbf{A}\mathbf{\Phi}\|_2^2, \quad (4)$$

where the second term is the usual sum-of-squares ℓ_2 norm of the error in reproducing the training data (in this case, DFT forces). The ℓ_1 term drives the model towards solutions with a small number of nonzero FCT elements, and the parameter μ is used to adjust the relative weights of the ℓ_1 and ℓ_2 terms. Higher values of μ will produce a least-square like fitting at the expense of denser FCTs that are prone to over-fitting, while small μ will produce very sparse under-fitted FCTs, simultaneously degrading the quality of the fit. The main advantage of CLSD over other methods for model building is that it does not require prior physical intuition to pick out potentially relevant FCTs and the fitting procedure is very robust with respect to noise, both random numerical noise in the DFT forces and systematic noise due to physical interactions that have been left out of the chosen model.

Full account of the technical details of our approach will be given in a separate publication, and here we only describe the key features of our method. The optimal value of μ that produces a model with the highest predictive accuracy lies between the aforementioned extremes and can be determined by monitoring the predictive error for a leave-out subset of the training data which is not used in Eq. (4) [24]. The predictive accuracy of the resulting model is then validated on a third, distinct set of DFT data, which we refer to as the "prediction set". The problem is scaled by $\Phi \to \Phi u_0^{n-1}$ and $u \to u/u_0$, where n is the order of the FCT and u_0 is a "maximum" displacement chosen to be on the order of the amplitude of thermal vibrations; this guarantees that all the terms in the ℓ_1 norm have the same unit of force, and helps improve the mutual coherence of the sensing matrix $\mathbf{A}$ [30]. Space group symmetry and translational invariance conditions are used to reduce the number of independent FCT elements [29]; the latter are also important for momentum conservation according to the Noether's theorem. These

linear constraints are applied algebraically by constructing a null-space matrix. Since the Taylor expansion employs non-orthogonal and unnormalized basis functions u^n, it is challenging to construct training configurations that would ideally satisfy the so-called incoherence requirement for the sensing matrix $\mathbf{A}$ [19]. As a result, we require a a relatively large training set compared to those used for the orthogonal basis in CS cluster expansion [24]. However, this is not a serious practical limitation because a large number of independent forces $(3m-3)$ can be extracted from each m-atom supercell configuration. Note that optimal compressive sensing favors configurations with random atomic displacement, while the physically accessible configurations follow thermodynamic distributions. In practice molecular dynamics (MD) trajectories (at temperatures of interest) each with random displacement (~ 0.2 Å) added to every atom were found sufficient for CSLD.

To demonstrate the efficiency and accuracy of CSLD, we use it to study anharmonic phonon dynamics and thermal conductivity in $Cu_{12}Sb_4S_{13}$, a compound related to an earth-abundant natural mineral tetrahedrite, which has been recently shown to be a high-performance thermoelectric [31, 32]. Experiment found very low lattice thermal conductivity of $\lesssim 1$ W/mK in the undoped sample, and our previous calculation showed the presence of unstable phonon modes [31], both point to strong anharmonicity. The body-centered cubic (bcc) $Cu_{12}Sb_4S_{13}$ (space group $I\bar{4}3m$) has 29 atoms in the primitive cell, a fairly large number that complicates computation of FCTs. For example, there are 188 distinct atomic pairs within a radius of $a = 10.4$ Å, 116 triplets within $a/2$, and so on. Taking into account the 3^n elements of each tensor, the number of coefficients N explodes quickly (55584 in our setting). After symmetrization, $N = 3188$ still represents a formidable numerical challenge.

DFT calculations were performed using the Perdew-Becke-Ernzerhof (PBE) functional [33], PAW potentials [34], a cutoff energy of 600 eV, and no symmetry constraints as implemented in the VASP code [35]. The training set consists of a) two $2a \times 2a \times 2a$ bcc supercell structures with the $3 \times 3 \times 3$ k-point grid and all atoms randomly displaced by up to 0.2 Å, and b) 70 *ab initio* MD trajectory snapshots with a bcc supercell and a $6 \times 6 \times 6$ k-point grid, taken at 3 ps intervals, at each of $T = 100, 200, \cdots, 700$ K.

Due to the considerable memory footprint of treating the $M \times N$ matrix A, the CSLD model optimization went through two stages. First, about $N = 3 \times 10^4$ ($\sim 5 \times 10^5$ before symmetrization) FCT elements up to 6th order were fitted with CS (eq. 4). Those tensors with all zero or near-zero elements as predicted by compressive sensing were filtered out. The remaining 443 tensors are overall physically meaningful, including 1) pair interactions, 2) bond bending, e.g. S-Cu-S, and 3) high order derivatives, e.g. $\partial^4 V/\partial u_x^4$. Next, the final candidates of $N = 3192$ elements, including 4, 1382, 389, 787, 224, 406 at the 1st–6th order, respectively, are fitted again. The optimized fitting parameters are $\mu = 27$ Å/eV and $u_0 = 0.6$ Å.

Fig. 1 shows the overall accuracy in the obtained CSLD model over a $2 \times 2 \times 2$ bcc structure not included in the fitting. Here all atoms are randomly displaced by 0.3 Å. The root-mean-square (rms) error of the force components compared to DFT values is 0.08 eV/Åand the relative error is 3%.

Fig. 2 clearly demonstrates the strong anharmonicity of $Cu_{12}Sb_4S_{13}$. The phonon dispersion (fig. 2a) according to pair force constants extracted by CSLD features unstable modes and is in good agreement with our previous calculation with LDA linear response [31], confirming the validity of CSLD at the harmonic level. Out of 1382 pair coefficients considered, CSLD picks out a sparse solution of 154 non-zero ones. Fig. 2b shows the DFT potential energy surface (points) along an unstable Γ point mode of predominant Cu(2) displacement out of the plane of three Cu(2)-S bonds (inset). The double-well behavior of this potential energy surface points to strong anharmonicity and high-order FCTs. Our CSLD model (lines) is able to reproduced the potential energy within 2 meV.

To test the applicability of this method in calculating lattice thermal conductivity, simulations were performed on the well-studied NaCl in addition to tetrahedrite. Force constants for both systems were generated using the above procedure. We developed a MD program (LMD) using Eq. 1 as the potential . Multiple popular methods were implemented for calculating thermal conductivity, including Green Kubo [36, 37], reverse non-equilibrium MD (RNEMD)[38] and homogenous non-equlibrium MD (HNEMD)[39].

After extensive testing of these methods we found HNEMD to be the most reliable. This method works by subjecting the system to an external field, $\mathbf{F}_e$, which is used to modify the equations of motion such that the force on atom a is given by

$$\mathbf{F}_a = F_a - \sum_b \mathbf{F}_{ab} \left(\mathbf{r}_{ab} \cdot \mathbf{F}_e\right) + \frac{1}{N} \sum_{b,c} \mathbf{F}_{bc} \left(\mathbf{r}_{bc} \cdot \mathbf{F}_e\right) \quad (5)$$

where F_a is the unmodified force calculated from Eq. 2. The external field has the effect of driving higher energy (hotter) particles with the field and lower energy (colder) particles against the field, while a thermostat is used to remove the heat generated from the work done by the external field. This results in an non-zero average heat flux, in the absence of a temperature gradient, which is given by

$$\langle \mathbf{J}(t) \rangle = -\beta V \int_0^t ds \, \langle \mathbf{J}(t-s)\mathbf{J}(0) \rangle \cdot \mathbf{F}_e \quad (6)$$

When the external field is zero, the above equation gives the equilibrium value of the average heat flux. Setting the external field to $\mathbf{F}_e = (0, 0, F_z)$ and in the limit that $t \to \infty$ we get the following relation

$$k = \frac{V}{k_B T^2} \int_0^\infty dt \, \langle J_z(t) J_z(0) \rangle = \lim_{F_z \to 0} \frac{-\langle J_z(\infty) \rangle}{T F_z} \qquad (7)$$

The process then involves a series of simulations at varying external fields $\mathbf{F}_e$ and constant T, with a simple linear extrapolation to zero field resulting in the true thermal conductivity.

Simulations were carried out for NaCl over a range of temperatures from 100K to 300K, with system sizes ranging from 512 to 4096 atoms. The lengths of the simulations ranged from 100 picoseconds to 1 nanosecond and all used a timestep of 1 fs. At each temperature a minimum of four different values for external field were used. The results obtained via this method are shown for NaCl in Fig. 3 (a). Extremely good agreement is seen between values determined from LMD and those obtained experimentally across the entire temperature range tested. Additionally, Fig. 3 (b) shows that there is no discernible size-dependence in the range of supercells tested.

Similar thermal conductivity simulations were done for tetrahedrite. Note that to simulate the relatively soft covalent bonds in tetrahedrite, we had to add a smoothed constraining wall on the bonds to prevent complete bond dissociation. Unlike NaCl, however, relatively little data is available on the thermal conductivity of tetrahedrite. Recent work by Lu, et. al. suggests a low-temperature lattice thermal conductivity of less than $1 W/mK$ [40]. LMD simulations result in a thermal conductivity of $0.38 \pm 0.04 W/mK$ for tetrahedrite at 100K.

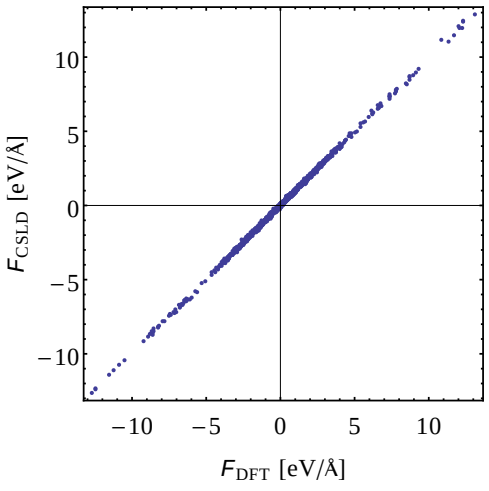

FIG. 1. Comparison of CSLD predicted and DFT force components when all atoms are randomly displaced by 0.3 Å.

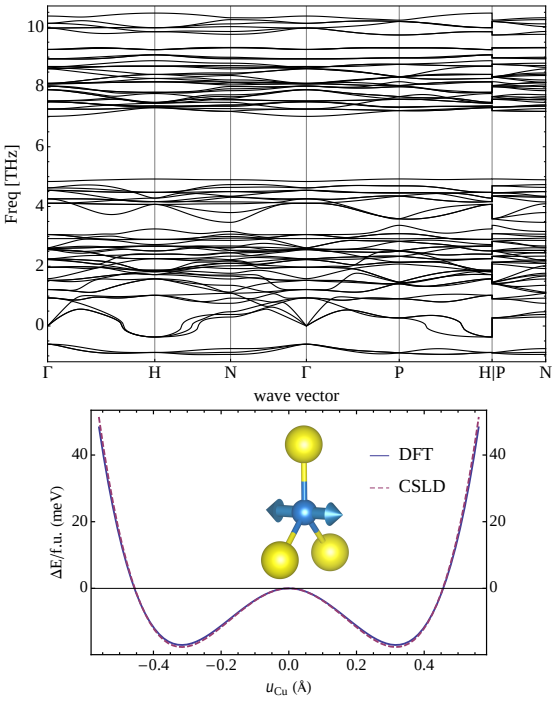

FIG. 2. Anharmonicity of tetrahedrite. (a) Phonon dispersion from CSLD. (b) Energy per $Cu_{12}Sb_4S_{13}$ relative to equilibrium from DFT (dots) and CSLD (line) of an unstable optical mode dominated by out-of-plane Cu displacement.

In conclusion, we proposed a general approach to lattice dynamics. The main methodological advance proposed here is the use of compressive sensing to automatically construct high-order anharmonic lattice Hamiltonians from DFT calculations. CSLD is more general and straight-forward than the existing methods for treating anharmonicity. For instance, CSLD can easily include 4–6 th-order anharmonicity (important for many cubic systems with double-well type potentials), which is inaccessible to DFPT . CSLD does not require special electronic structure codes, but can be used directly with highly accurate, established DFT codes , and can be implemented in an automated manner. The model accuracy may be improved systematically through the robust framework of compressive sensing. This technical development is a big step towards automated calculations of lattice dynamics for a wide variety of materials, enabling systematic studies of thermal properties for hundreds, maybe thousands of compounds.

The authors gratefully acknowledge financial support for method and code development from the National Science Foundation under Award Number DMR-1106024. Calculations related to $Cu_{12}Sb_4S_{13}$ were performed as part of the Center for Revolutionary Materials for Solid State Energy Conversion, an Energy Frontier Research Center funded by the U.S. Department of Energy, Office of Science, Office of Basic Energy Sciences under Award Number DE-SC0001054. Part of the work by

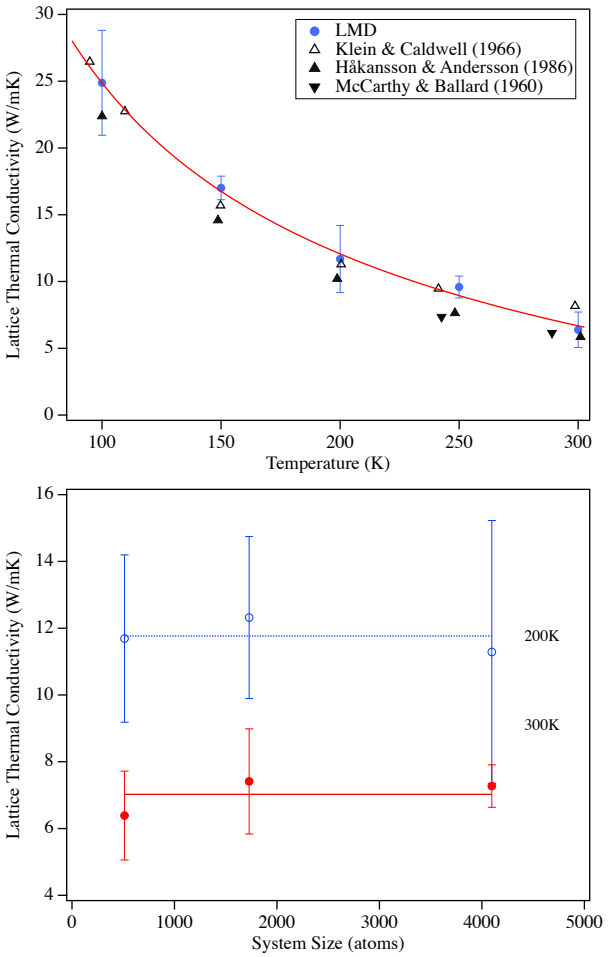

FIG. 3. Thermal conductivity of NaCl. (a) Lattice thermal conductivity over a range of temperatures, circles are computational results from the present study, triangles are experimental data from [41–43] and the line is a power fit of the simulation results. (b) System size dependence. The lines are averages of the three values.

F.Z. was performed under the auspices of the US DOE by Lawrence Livermore National Laboratory under Contract DE-AC52-07NA27344. We used computing resources at the National Energy Research Scientific Computing Center, which is supported by the US DOE under Contract No. DE-AC02-05CH11231.

[1] M. Born and K. Huang, *Dynamical Theory of Crystal Lattices*, International series of monographs on physics (Oxford University Press, Oxford, 1954).
[2] H. Wendel and R. Martin, Physical Review Letters **40**, 950 (1978).
[3] K. M. Ho, C. L. Fu, and B. N. Harmon, Physical Review B **29**, 1575 (1984).
[4] K. Kunc and R. M. Martin, Physical Review Letters **48**, 406 (1982).
[5] K. Parlinski, Z. Li, and Y. Kawazoe, Physical Review Letters **78**, 4063 (1997).
[6] S. Baroni, S. de Gironcoli, A. Dal Corso, and P. Giannozzi, Reviews Of Modern Physics **73**, 515 (2001).
[7] G. Horton and A. Maradudin, *Dynamical Properties of Solids: Crystalline solids, fundamentals*, Dynamical Properties of Solids (North-Holland Publishing Company, 1974).
[8] N. R. Werthamer, Physical Review B **1**, 572 (1970).
[9] A. A. Maradudin, A. E. Fein, and G. H. Vineyard, physica status solidi (b) **2**, 1479 (1962).
[10] M. Omini and A. Sparavigna, Physical Review B **53**, 9064 (1996).
[11] A. Debernardi, S. Baroni, and E. Molinari, Physical Review Letters **75**, 1819 (1995).
[12] D. A. Broido, M. Malorny, G. Birner, N. Mingo, and D. A. Stewart, Applied Physics Letters **91**, 231922 (2007).
[13] J. Garg, N. Bonini, B. Kozinsky, and N. Marzari, Physical Review Letters **106**, 045901 (2011).
[14] K. Esfarjani, G. Chen, and H. T. Stokes, Physical Review B **84**, 085204 (2011).
[15] P. Souvatzis, O. Eriksson, M. I. Katsnelson, and S. P. Rudin, Physical Review Letters **100**, 095901 (2008).
[16] O. Hellman, I. A. Abrikosov, and S. I. Simak, Physical Review B **84** (2011).
[17] O. Hellman and I. A. Abrikosov, Physical Review B **88**, 144301 (2013).
[18] X. Gonze and C. Lee, Phys. Rev. B **55**, 10355 (1997).
[19] E. Candès and M. Wakin, Signal Processing Magazine, IEEE **25**, 21 (2008).
[20] K. Esfarjani and H. Stokes, Physical Review B **77**, 144112 (2008).
[21] X. Gonze and C. Lee, Physical Review B **55**, 10355 (1997).
[22] J. Sanchez, F. Ducastelle, and D. Gratias, Physica A **128**, 334 (1984).
[23] D. de Fontaine, in *Solid State Physics*, Vol. 47, edited by H. Ehrenreich and D. Turnbull (Academic, New York, 1994).
[24] L. J. Nelson, G. L. W. Hart, F. Zhou, and V. Ozoliņš, Physical Review B **87**, 035125 (2013).
[25] L. J. Nelson, V. Ozoliņš, C. S. Reese, F. Zhou, and G. L. W. Hart, Physical Review B **88**, 155105 (2013).
[26] E. J. Candès and T. Tao, Information Theory, IEEE Transactions on **51**, 4203 (2005).
[27] E. J. Candès, J. K. Romberg, and T. Tao, Communications on Pure and Applied Mathematics **59**, 1207 (2006).
[28] E. J. Candès, J. Romberg, and T. Tao, Information Theory, IEEE Transactions on **52**, 489 (2006).
[29] G. K. Horton and A. A. Maradudin, eds., *Dynamical Properties of Solids: Crystalline solids, fundamentals*, Dynamical Properties of Solids (North-Holland, Amsterdam, 1974).
[30] D. L. Donoho and X. Huo, IEEE Trans. Inform. Theory **47**, 2845 (2001).
[31] X. Lu, D. T. Morelli, Y. Xia, F. Zhou, V. Ozolins, H. Chi, X. Zhou, and C. Uher, Adv. Energy Mater. **3**, 342 (2012).
[32] K. Suekuni, K. Tsuruta, T. Ariga, and M. Koyano, Appl. Phys. Express **5**, 051201 (2012).
[33] J. Perdew, K. Burke, and M. Ernzerhof, Phys. Rev. Lett. **77**, 3865 (1996).
[34] P. Blochl, Phys. Rev. B **50**, 17953 (1994).
[35] G. Kresse and D. Joubert, Phys. Rev. B **59**, 1758 (1999).

[36] M. S. Green, The Journal of Chemical Physics **22**, 398 (1954).
[37] R. Kubo, Journal of the Physical Society of Japan **12**, 570 (1957).
[38] F. Müller-Plathe and P. Bordat, "Reverse non-equilibrium molecular dynamics," in *Novel Methods in Soft Matter Simulations*, Lecture Notes in Physics, Vol. 640, edited by M. Karttunen, A. Lukkarinen, and I. Vattulainen (Springer Berlin Heidelberg, 2004) pp. 310–326.
[39] D. J. Evans, Physics Letters A **91**, 457 (1982).
[40] X. Lu, D. T. Morelli, Y. Xia, F. Zhou, V. Ozolins, H. Chi, X. Zhou, and C. Uher, Advanced Energy Materials **3**, 342 (2013).
[41] B. Håkansson and P. Andersson, Journal of Physics and Chemistry of Solids **47**, 355 (1986).
[42] M. V. Klein and R. F. Caldwell, Review of Scientific Instruments **37**, 1291 (1966).
[43] K. A. McCarthy and S. S. Ballard, Journal of Applied Physics **31**, 1410 (1960).